

The effect of injection pressure and fuel viscosity on the spray characteristics of biodiesel blends injected into an atmospheric chamber[†]

Ainul Ghurri^{1,2}, Jae-Duk Kim², Hyung Gon Kim³, Jae-Youn Jung⁴ and Kyu-Keun Song^{4,*}

¹Department of Mechanical Engineering, Udayana University, Bali-Indonesia

²Graduate School, Precision Mechanical Eng., Chonbuk National University, 657 Baekje-daero Deokjin-Gu Jeonju-si Jeollabuk-do 561-756, Korea

³School of Mechanical System Engineering, Chonbuk National University, 657 Baekje-daero Deokjin-Gu Jeonju-si Jeollabuk-do 561-756, Korea

⁴RCIT, Chonbuk National University, 657 Baekje-daero Deokjin-Gu Jeonju-si Jeollabuk-do 561-756, Korea

(Manuscript Received June 14, 2011; Revised January 12, 2012; Accepted April 13, 2012)

Abstract

An experimental study was conducted to examine the effect of injection pressure and fuel type on the spray tip penetration length and the angle of spray injected into atmospheric chamber. The objective of the present study is to formulate empirical correlations of the spray tip penetration and the spray angle for non-evaporative condition. The experiment was performed by a common rail type high-pressure injector for the diesel engine at the injection pressure 40~100 MPa and four different fuels (D100, BD25, BD45, and BD65). The results showed that the biodiesel content increased the spray tip penetration and decreased the spray angle. The correlation of spray tip penetration is expressed for each region before and after spray break-up time in terms of injection pressure, fuel viscosity and time after start of injection. The correlation is also obtained for spray angle equation terms of injection pressure and fuel viscosity.

Keywords: Common rail; Spray angle; Spray correlation; Spray tip penetration

1. Introduction

There are a lot of works that have been published on fuel spray characteristics both experimentally. Many of them proposed the spray equations -mainly spray penetration and spray angle-based on the experimental results. While the experimental results have showed a generally acceptable conclusion; there are quite different results as expressed in their equations. For example, in the spray-angle equation that expressed as a function of air to fuel density, the exponent of air to fuel density varied among different authors, i.e. 0.26 by Hiroyasu and Arai [1], 0.19 by Naber and Siebers [2], and 0.5 by Arregle et al. [3], respectively.

Hiroyasu and Arai [1] concluded that the time-dependent development of spray penetration length S can be divided into two phases. The first phase starts at the beginning of injection when the needle begins to open and ends when the liquid jet appearing from the nozzle hole starts to disintegrate ($t = t_{break-up}$). During the first phase, a linear growth of S along t (time after start of injection) can be observed. At the second phase ($t > t_{break-up}$), the spray tip consists of droplets, and the tip velocity is smaller than the first phase [4]. The

spray tip continues to penetrate into the ambient due to the new droplets with high kinetic energy that follow in the wake of the slower droplets at the tip, and replacing those slower droplets [4]. It is interest to note that in second phase of injection the slope of the S along with t is half of the first phase [5]. Nabers and Siebers [2] reported the significant effect of gas density to decrease the penetration, while the vaporization resulted in decreasing spray penetration and dispersion by as much as 20% relative to non-vaporizing conditions. Arregle et al. [3] validated and extended some correlations for the sprays generated by common-rail system that involved similar parameters i.e. ΔP , d_o , ρ_a , and t . Later some authors developed further to investigate the effect of several injection parameters and injector geometry on the spray characteristics; and generally reported the well-agreement results to the established correlations [6-8]. Sazhin et al. proposed analytical correlations for spray penetration derived for the initial stage of injection and two-phase flow regime that gives more accurate predictions compared to some proposed earlier [9]. Song et al. [10] formulated spray penetration and angle equations for their injection system using single-hole injector, and showed well-agreement results to the earlier correlations. Recently, reports on spray characteristics have developed to wider area in related to the alternatives for diesel fuel like DME and biodiesel [11, 12], the use of numerical study to predict the spray characteristics [13, 14], and also in digital

*Corresponding author. Tel.: +82 63 270 2376, Fax.: +82 63 270 2388
E-mail address: songkk@jbnu.ac.kr

[†]Recommended by Associate Editor Kyoung Dong Min

© KSME & Springer 2012

imaging process of the spray [15, 16]. Generally, the results are conclusive about the trend of spray tip penetration and spray angle as described in earlier papers, and some of them used well-known correlations such as Dent's, Hiroyasu's, Arregle's and Sazhin's as comparison to the experimental results [16-18]. The experimental parameters commonly used various conditions in injection pressure, ambient pressure and temperature, and different kind of injection system. The experimental correlations are then expressed with all or partly of these parameters: ΔP , d_o , ρ_a , t and θ , etc. It is important to note that most of correlations formulated from spray injected into high-pressure chamber with or without evaporative conditions as effort to close to the in-cylinder condition. When comparing the existing correlations to the experimental data of spray injected into atmospheric conditions, Suh and Lee [11] found that the spray tip penetration suggested by Hiroyasu and Arai [1] underestimated to that of experimental result. On the other hand, Sazhin empirical results [9] overestimated the spray tip penetration under atmospheric conditions especially at the early stage of injection. Ghurri et al. also reported that Hiroyasu & Arai correlations underestimated the experimental data of spray injected into an atmospheric chamber at injection pressure 90 MPa especially beyond 0.8 ms after start of injection [19].

The present work formulated the spray tip penetration correlations from the experimental data of fuel injected into an atmospheric chamber by using common-rail injection system for various fuels (D100, BD25, BD45, and BD65, respectively). The spray angle correlation was also formulated in terms of injection pressure and fuel viscosity.

2. Experimental facilities

Fig. 1 displays the experimental set up consisting of a fuel tank, feed pump, fuel filter, high pressure pump driven by DC motor, common rail injection system, and an electronic high speed video camera to capture the spray images. The fuel properties and experimental conditions are described in Tables 1 and 2.

Fuel temperature in the fuel tank was maintained constantly. Fuel was fed by a feed pump to pass a fuel filter and drawn by a DC motor-driven high pressure pump. The 3.7 kW DC motor could be adjusted up to 3000 rpm in speed. The high-pressure fuel was then delivered to the injector via the common rail. One part of the fuel was injected into a quiescent atmospheric chamber at room temperature; the other part controls the injection nozzle of the injector and then flowed back to the tank. Pressure sensors measured the fuel pressure in the rail. This signal was compared to a desired value adjusted in a controller drive (TEMS, TDA 1100H).

The injection could be controlled internally or externally by an injector drive (TEMS, TDA 3200H). The injected fuel quantity was determined by the duration of injection, fuel pressure in the rail, and the flow area of the injector. Spray images were captured by a high-speed camera (FASTCAM

Table 1. Fuel properties.

Fuel properties	Diesel (D100)	Biodiesel
Density (kg/m ³)	850	884
Viscosity (mm ² /s)	3.25	4
Flash point (°C)	68	139
Pour point (°C)	-35 ÷ -15	0
Cetane number	54.6	54 ÷ 56

Table 2. Experimental condition.

Injection system	Common-rail
Injector needle	5 side holes
Hole diameter	0.2 mm
Injection duration	1000 μ s
Injection pressure	40 ÷ 100 MPa
Ambient gas	Atmospheric air
Ambient temperature	285 K
High speed camera	FASTCAM Ultima40k
Frame rate	9000 fps
Resolution	256 x 128

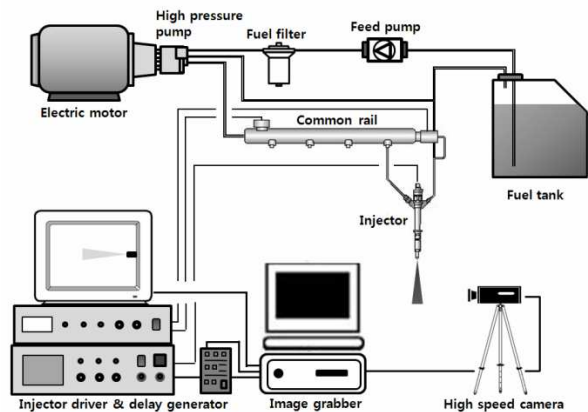


Fig. 1. The experimental apparatus.

Ultima40k) with a metal-halide lamp as a light source. A multi-channel digital delay/pulse generator and an image grabber connected to a computer were used to synchronize the fuel injection and camera shutter signal.

A five-hole nozzle injector having 0.2 mm diameter and a 156° spray angle was used in this experiment. The spray images were taken at a shutter speed of 18000 FPS and used black as the background screen. The present work performed the experiments at injection pressure 40–100 MPa, respectively, and 1000 μ s of injection duration for each injection pressure. The fuels used in the experiment were D100, BD25, BD45 and BD65 respectively.

3. Results and discussion

The spray images series of this experiment until 1.87 ms after start of injection (ASOI) are presented in Fig. 2, while the spray structure is defined as shown in Fig. 3. Spray tip penetration is measured from nozzle tip to the furthest spray pixel. The spray angle is measured as the angle between the tangents

Table 3. Injected fuel quantity.

Injection pressure (MPa)	Injection duration (μ s)	Injected volume ($\text{mm}^3/\text{injection}$)
30	1000	14.1
60	1000	23.5
90	1000	37.6

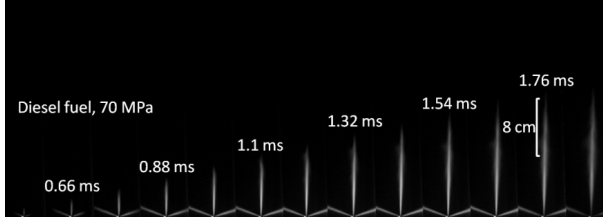


Fig. 2. Spray image series.

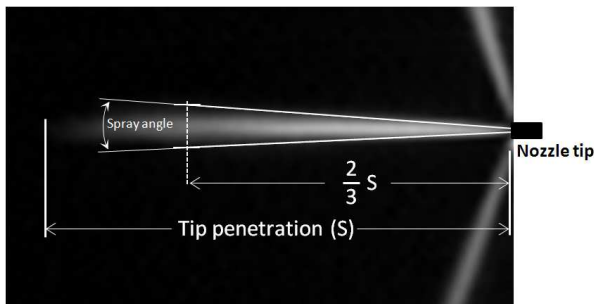


Fig. 3. Spray tip penetration and angle.

to the spray envelope in the region up to $2/3$ of penetration length.

The fuel quantity injected at injection pressure 30, 60 and 90 MPa is presented in Table 3. Generally the injection rate increased during 0.5 ms of early stage of injection and then decreased until the end of injection.

3.1 Spray tip penetration

Fig. 4 shows the spray tip penetration (STP) of various fuels at injection pressure 70 MPa, while Fig. 5 shows the STP of D100 at injection pressure 50, 70, and 90 MPa, respectively, presented in linear scale. It is shown that the spray tip penetration developed along with time after start of injection. The effect of fuel type can be seen in Fig. 4, while the effect of injection pressure is clearly observed that the higher injection pressure resulted in the longer spray tip penetration as shown in Fig. 5. Figs. 6 and 7 shows the spray tip penetration corresponded to Figs. 4 and 5 that are presented in logarithmic scale. The STP in logarithmic scale shows the evolution of spray tip penetration with two different slopes that couldn't be observed in the linear scale. In the first stage, the spray tip penetration increased quickly, and then the slope decreased around the half of the first stage. The change time of the slope is recognized as the break-up time of the spray. As shown in Fig. 7, the spray injected in higher injection pressure had earlier break-up time. As for the STP of various fuels at the same

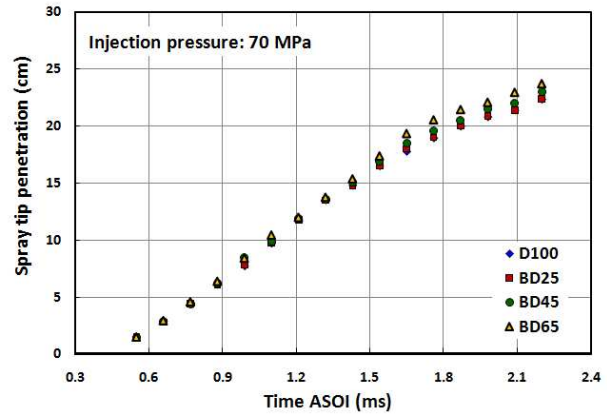


Fig. 4. STP of various fuels at same injection pressure.

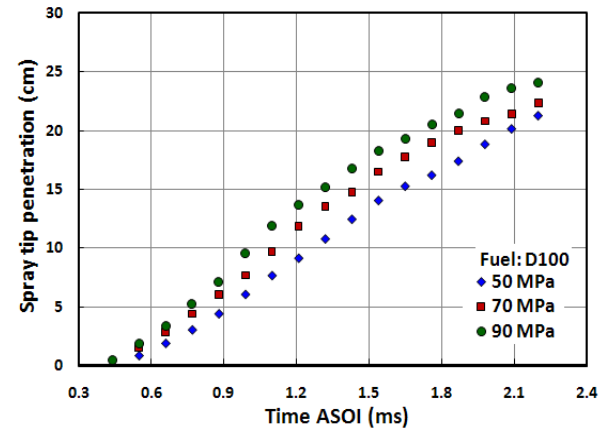


Fig. 5. STP D100 at various injection pressure.

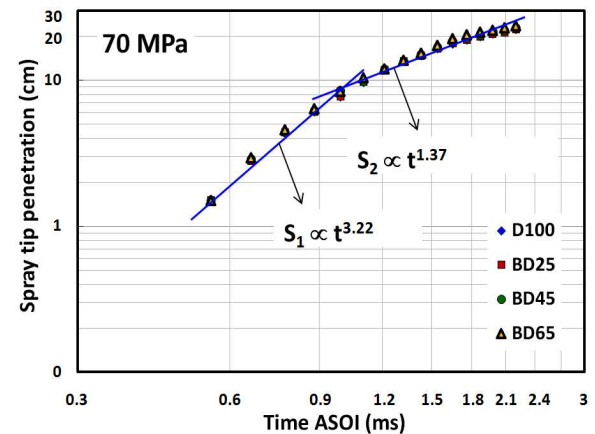


Fig. 6. The STP of various fuels in logarithmic scale.

injection pressure, the difference of STP became more difficult to observe visually in the graph.

The empirical equation would have been formulated for the spray tip penetration before and after the break-up time. The spray tip penetration would be expressed as:

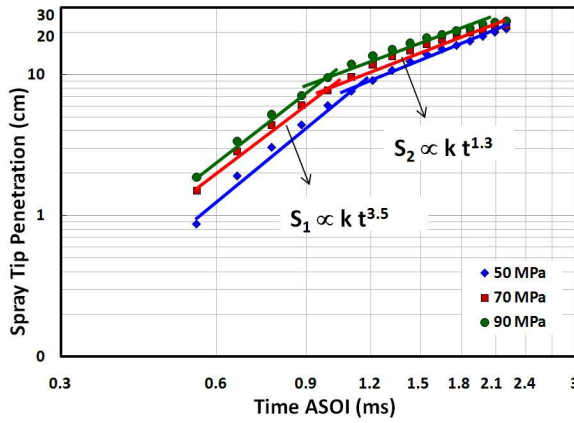


Fig. 7. The STP of D100 in logarithmic scale.

$$S = f(P_a, P_{in}, \nu, t) \tag{1}$$

or

$$S = f(\Delta P, \nu, t). \tag{2}$$

S is spray tip penetration, P_a is ambient pressure, P_{in} is injection pressure, ΔP is $P_{in} - P_a$, ν is liquid fuel viscosity, and t is temporal time after start of injection. The correlation excluded the air density since this experiment was conducted in constant air density and constant atmospheric temperature.

In the logarithmic graph it could be plotted the straight power trend-lines to find the equations that fitted to the spray tip penetration data. In Figs. 6 and 7, it is also presented the equations of the spray tip penetration for each injection pressure as function of time after start of injection (t). In Fig. 6, it is shown the average value of exponent for t as the effect of fuel viscosity. The constant k in Fig. 7 is a function contained the effect of fuel viscosity and the injection pressure. The power trend-lines fitted very well to the data with coefficient of determination ranged from 87.3% to 99.9%. S_1 and S_2 denoted the spray tip penetration before and after break-up time, respectively.

By examining the effect of injection pressure, Fig. 7 produced the spray tip penetration function as follows:

$$S_1 = k t^{3.5} \quad \text{for } 0 < t < t_b \tag{3}$$

$$S_2 = k t^{1.3} \quad \text{for } t > t_b \tag{4}$$

where t_b is break-up time.

The constant k can be expressed as a function of the momentum of spray and the fuel viscosity. The k was then determined for each region before and after break-up time to formulate the effect of fuel viscosity as shown in Figs. 8 and 9, respectively. The value of k was found as follows:

$$k = k_1 \nu^{0.54} \quad \text{for } 0 < t < t_b \tag{5}$$

$$k = k_1 \nu^{0.17} \quad \text{for } t > t_b. \tag{6}$$

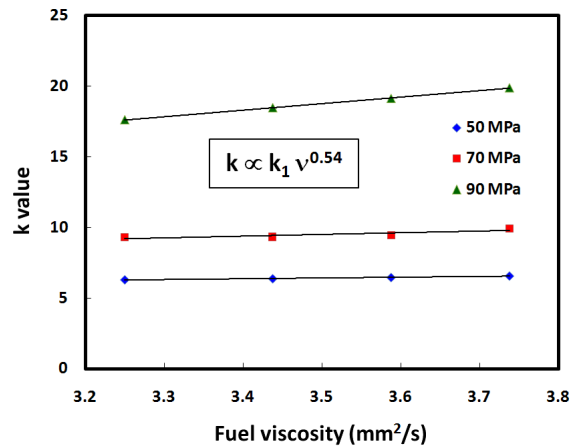


Fig. 8. The value of k before t_b .

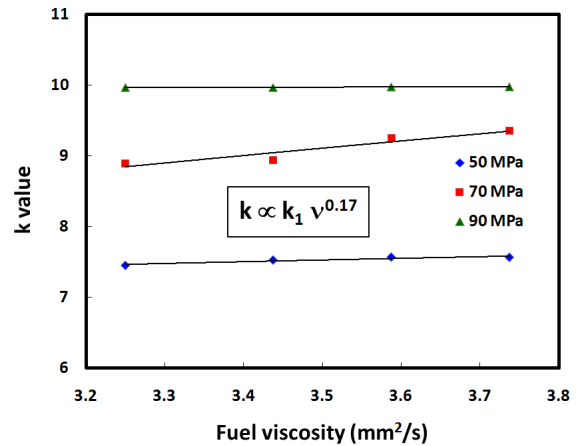


Fig. 9. The value of k after t_b .

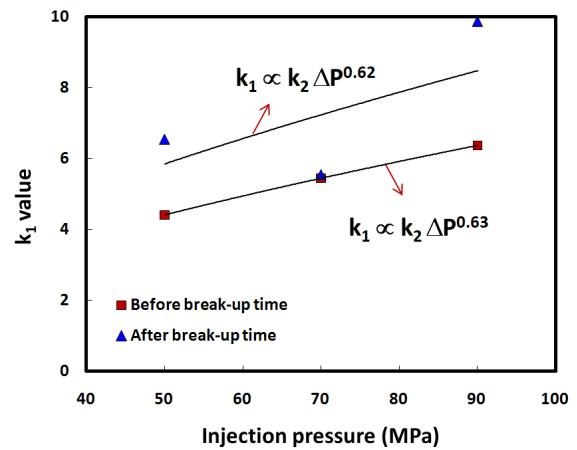


Fig. 10. The value of k_1 for each injection pressure.

Finally, by examining k_1 values for each injection pressure, the function between k_1 and the injection pressure could be concluded as shown in Fig. 10 as follows:

$$k_1 = k_2 \Delta P^{0.62} \quad \text{for } 0 < t < t_b \tag{7}$$

$$k_1 = k_2 \Delta P^{0.63} \quad \text{for } t > t_b. \tag{8}$$

The empirical correlations from the present experiment then could be formulated as follows:

$$S_1 = 0.38\Delta P^{0.62}v^{0.54}t^{3.5} \quad \text{for } 0 < t < t_b \quad (9)$$

$$S_2 = 0.49\Delta P^{0.63}v^{0.17}t^{1.32} \quad \text{for } t > t_b \quad (10)$$

From Eqs. (9) and (10) it is seen that the spray tip penetration grows along time after start of injection (t) much quicker before break-up time; more than 2 times that of after break-up time. The exponents of time are very different to those of the previous results [1-3, 6, 10]. These exponents in the present work are very high i.e. 3.5 and 1.32 for S_1 and S_2 , respectively, (compared to 1 and 0.5 at the previous results). The exponent of time for S_2 is around 2.65 times of that of S_1 , compared to 2.5 times in the previous results. These may correspond to the very short injection duration applied in the present work. In the present work, the injection duration is 1 ms that is very short compared to the previous published papers. As the results, the spray tip penetration developed quickly because the high pressure energy of the fuel is transferred to the spray movement in very short time. The high exponents of time (i.e. 3.5 and 1.32) represent the quick evolution of spray tip penetration during this short injection duration. The other reason is the higher injection pressure applied in the present work that means the higher availability of energy to produce spray in very short injection duration.

The exponents of injection pressure are quite similar for both before and after break-up time. The injection pressure affected spray tip penetration at same level during the short injection duration. The role of fuel viscosity seems stronger before break-up time than that of after break-up time. Before the break-up time, the spray had larger droplet diameter that means higher momentum to penetrate the ambient air. As the results, the spray tip penetration developed quicker at the early stage of injection, and slower after the break up time when the spray atomization to the smaller droplet occurred. The most data showed the initial STP of D100 always longer than biodiesel fuel. This was caused by the higher initial velocity of the D100 spray as consequence of lower viscosity and density of the D100. The higher viscosity of biodiesel fuel resulted higher resistance to break-up. However the higher viscosity also enabled the spray to have the higher momentum of biodiesel fuel at further time after start of injection. As the result, the biodiesel spray could reach slightly longer penetration length compared to D100.

The plotting graphs both experimental and the calculated spray tip penetration by Eqs. (9) and (10) are shown in Fig. 11 for all injection pressures tested in the present work ranged from 40 to 100 MPa. The measured spray tip penetrations appeared to vary rather strongly with the time after start of injection. Nevertheless, the most of measured data deviates within $\pm 8\%$ from the calculated spray tip penetration, which is fairly well.

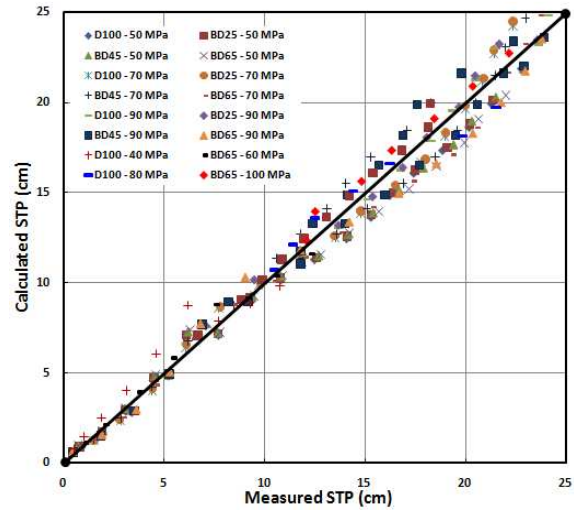


Fig. 11. Spray tip penetration equation's accuracy plot.

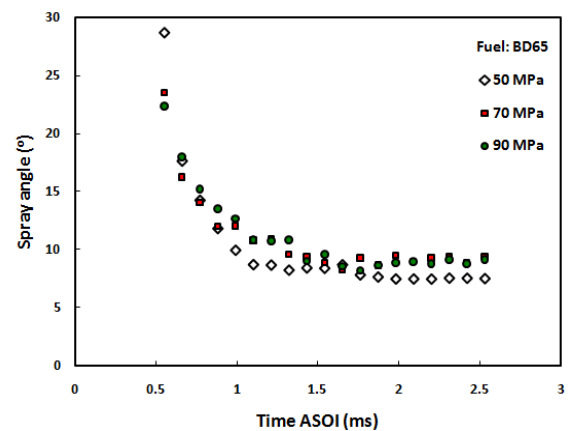


Fig. 12. The spray angle at different injection pressure.

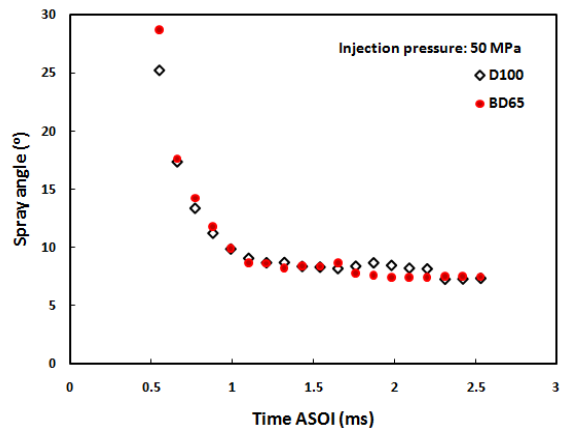


Fig. 13. The spray angle of different fuel types.

3.2 Spray angle

The experimental results of spray angle at different injection pressure and different fuel types are shown in Figs. 12 and 13, respectively. The spray angle decreased abruptly at early stage

of injection until around 1 ms and became independent of time after that.

The spray angle equation was then formulated used the average value of the spray angle after 1 ms on the basis of the liquid fuel viscosity and the injection pressure for the tested-fuels. The experimental correlation for the spray angle was found as follows:

$$\tan(\theta/2) = 0.15\Delta P^{0.017} \nu^{-0.7} \quad (11)$$

Eq. (11) showed a small effect of injection pressure to the spray angle. When examined the effect of injection pressure on the spray angle, Arregle et al. found the exponent for injection pressure was 0.00943 [3]. It could be concluded that the spray angle is mainly affected by fuel viscosity. The most authors reported the spray angle correlation for the evaporative experiment on the term of air to fuel density ratio [1-3, 6-8]; and showed the increase of fuel density -that means similarly with the viscosity- resulted in the decrease of the spray angle. The Eq. (11) showed a similar result in terms of fuel viscosity.

4. Conclusions

An experimental study was conducted to examine the effect of injection pressure and fuel type on the tip penetration length and the angle of spray injected into atmospheric chamber in order to formulate empirical correlations of the spray tip penetration and the spray angle for non-evaporative condition. The equation of spray tip penetration is expressed for each region before and after spray break-up time in terms of injection pressure, liquid fuel viscosity and time after start of injection. The spray angle equation is expressed in terms of injection pressure and liquid fuel viscosity. The correlations are expressed as follows:

Spray tip penetration:

$$S_1 = 0.38\Delta P^{0.62} \nu^{0.54} t^{3.5} \quad \text{for } 0 < t < t_b$$

$$S_2 = 0.49\Delta P^{0.63} \nu^{0.17} t^{1.32} \quad \text{for } t > t_b$$

Spray angle:

$$\tan(\theta/2) = 0.15\Delta P^{0.017} \nu^{-0.7} \quad .$$

The calculated results of spray tip penetration were compared to the experimental data for the injection pressure 40–100 MPa and the accuracy plot showed a fairly well agreement between them.

Acknowledgment

This paper was supported by the research funds of Chonbuk National University, 2011.

References

- [1] H. Hiroyasu and M. Arai, Structures of fuel sprays in diesel engine, *SAE Technical Paper Series*, 900475 (1990).
- [2] J. D. Naber and D. L. Siebers, Effects of gas density and vaporization on penetration and dispersion of diesel sprays, *SAE Technical Paper Series*, 960034 (1996).
- [3] J. Arregle, J. V. Pastor and S. Ruiz, The influence of injection parameters on diesel spray characteristics, *SAE Technical Paper Series*, 1999-01-00200.
- [4] C. Baumgarten, *Mixture formation in internal combustion engine*, Springer (2006).
- [5] A. H. Lefebvre, *Atomization and sprays*, Hemisphere Publishing Co. (1989).
- [6] S. Gupta, R. Poola and R. Sekar, Effect of injection parameters on diesel spray characteristics, *SAE Technical Paper Series*, 2000-01-1600 (2000).
- [7] R. Morgan, J. Wray, D. A. Kennaird, C. Crua and M. R. Heikal, The influence of injector parameters on the formation and break-up of a diesel spray, *SAE Technical Paper Series*, 2001-01-0529 (2001).
- [8] C. S. Bae, J. Yu, J. S. Kang, J. S. Kong and K. O. Lee, Effect of nozzle geometry on the common-rail diesel spray, *SAE Technical Paper Series*, 2002-01-1625 (2002).
- [9] S. S. Sazhin, G. Feng and M. R. Heikal, A model for fuel spray penetration, *Fuel*, 80 (2001) 2171-2180.
- [10] K. K. Song, S. C. Sim, B. K. Jung, H. G. Kim and J. H. Kim, Effect of injection parameters on diesel spray characteristics, *J Mech Sci Technol*, 19 (6) (2005) 1321-1328.
- [11] G. Yuan, D. Jun, L. Chunwang, D. Fengling, L. ZHuo, W. Zhijun and L. Liguang, Experimental study of the spray characteristics of biodiesel based on inedible oil, *Biotechnology Advance*, 27 (2009) 616-624.
- [12] J. K. Hyung, H. P. Su and S. L. Chang, A study on the macroscopic spray behavior and atomization characteristics of biodiesel and dimethyl ether under increased ambient pressure, *Fuel process technol*, 91 (2009) 354-363.
- [13] C. S. Lee and S. W. Park, An experimental and numerical study on fuel atomization characteristics of high-pressure diesel injection sprays, *Fuel*, 81 (2002) 2417–2423.
- [14] S. H. Park, H. J. Kim and C. S. Lee, Comparison of experimental and predicted atomization characteristics of high-pressure diesel spray under various fuel and ambient pressure, *J Mech Sci Technol*, 7 (2010) 1491-1499.
- [15] J. Shao, Y. Yan, G. Greeves and S. Smith, Quantitative characterization of diesel sprays using digital imaging techniques, *Meas. Sci. Technol*, 14 (2003) 1110-1116.
- [16] E. Delacourt, B. Desmet and B. Besson, Characterization of very high pressure diesel sprays using digital imaging techniques, *Fuel*, 84 (2005) 859-867.
- [17] J. D. Ryu, H. M. Kim and K. H. Lee, A study on the spray structure and evaporation characteristic of common rail type high pressure injector in homogeneous charge compression ignition engine, *Fuel*, 84 (2005) 2341–2350.
- [18] H. K. Suh and C. S. Lee, Experimental and analytical study

on the spray characteristics of dimethyl ether (DME) and diesel fuels within a common-rail injection system in a diesel engine, *Fuel*, 87 (2008) 925-932.

- [19] A. Ghurri, J. D. Kim, K. K. Song, J. J. Jung and H. G. Kim, Qualitative and quantitative analysis of spray characteristics of diesel and biodiesel blend on common-rail injection system, *J Mech Sci Technol*, 25 (4) (2011) 885-893.



Ainul Ghurri received the B.S. degree in mechanical engineering from Brawijaya University, Indonesia in 1995 and master degree in mechanical engineering from Indonesia University, Indonesia in 1998, respectively. He is a lecturer at mechanical engineering department of Udayana University, Indonesia. He is

currently a Ph.D. student in Precision Mechanical Engineering Department of Chonbuk National University, Jeonju, South Korea. His research interests are in the area of fuel spray characteristics, biodiesel fuel, and its engine performance and emissions characteristics.



Jae-Duk Kim received the B.S. and M.S. degrees in Precision Mechanical Engineering from Chonbuk National University, South Korea in 2009 and 2011. He is currently a Ph.D. student in Precision Mechanical Engineering Department of Chonbuk National University. His research interests include fuel spray injection characteristics, and diesel engine performance and emission characteristics.

tion characteristics, and diesel engine performance and emission characteristics.



Hyung Gon Kim received the B.S. and M.S. degrees in Precision mechanical Engineering from Chonbuk national University, Korea in 1995 and 1997; the Ph.D. degree from Kagoshima University, Japan in 2006. He currently works as an adjunct professor in Chonbuk National University. His current research interests are heat and fluid engineering, atomization system, and agricultural machinery.

research interests are heat and fluid engineering, atomization system, and agricultural machinery.



Jae-Youn Jung received the B.S. and M.S. degree in mechanical engineering from Chonbuk National University, South Korea and Ph.D. degree from Tokyo Institute of Technology, Japan. He is currently a professor at Precision Mechanical Engineering Department, Chonbuk National University. His major research field includes tribology, hydraulic pump and motor design, and its performance improvement.

major research field includes tribology, hydraulic pump and motor design, and its performance improvement.



Kyu-Keun Song received the B.S. and M.S. degree in mechanical engineering from Chonbuk National University, South Korea and Ph.D. degree in mechanical engineering from Hokkaido University, Japan. He is currently a professor at Precision Mechanical Engineering Department, Chonbuk National University. His research interests include combustion and exhaust emission characteristics of diesel engine, spray characteristics of biodiesel in common rails injection system.

University. His research interests include combustion and exhaust emission characteristics of diesel engine, spray characteristics of biodiesel in common rails injection system.